Title

Dispersion Effects in Spiral Phase Plate LG01 Generation and Consequences for FEL Laser Heating

Author

Zhou, Tina

Publication Date

2025-12-11

Dispersion Effects in Spiral Phase Plate LG_{01} Generation and Consequences for FEL Laser Heating

Tina Zhou

Department of Electrical and Computer Engineering, University of California, Los Angeles

ABSTRACT

Tang et al. [1] showed that an LG_{01} laser heater improves microbunching suppression in FELs. We analyze how SPP material dispersion changes the LG_{01} phase, causes OAM leakage, distorts the donut profile, and affects heater performance.

INTRODUCTION

Free-electron lasers (FELs) are powerful, tunable light sources that enable ultrafast imaging, molecular dynamics studies, and nanoscale material characterization. [2] Their performance depends strongly on electron-beam quality, so understanding and mitigating beam instabilities is essential for scientific and industrial applications.

Microbunching instability (MBI) is a collective effect in electron beams. During bunch compression, small density and energy fluctuations can grow and make the free-electron laser (FEL) spectrum worse. [2,3] A common way to reduce MBI is to use a laser heater. In a laser heater, a co-propagating laser overlaps with the electron beam in a short undulator and adds a controlled, uncorrelated energy spread.

Tang et al. [1] did experiments at LCLS and found that using a Laguerre–Gaussian LG_{01} beam instead of a TEM_{00} Gaussian beam gives a much smoother energy modulation. [1] In their setup, the electron beam is placed near the dark center of the LG_{01} donut. Near the center, the LG_{01} field increases roughly linearly with radius. When this field interacts with a transverse Gaussian electron distribution, the resulting energy spread becomes closer to a Gaussian shape, which helps to suppress microbunching more effectively.

In the Tang et al. [1] experiment, the LG_{01} beam is generated by a spiral phase plate (SPP). An ideal SPP with topological charge $l = 1$ applies an azimuthal phase factor $e^{i\theta}$, so it converts an incoming Gaussian beam into an optical vortex with charge one. [4,5] Physically, the SPP is a transmissive optic whose thickness $t(\theta)$ depends on the angle θ. For a plane wave with wavelength λ, the geometric phase is

$$\phi(\theta, \lambda) = \frac{2\pi}{\lambda} \left[n(\lambda) - 1\right] t(\theta), \tag{1}$$

where $n(\lambda)$ is the refractive index of the plate material. [5] The design condition $\phi(2\pi, \lambda_0) = 2\pi$ is satisfied only at the wavelength λ_0. For $\lambda \neq \lambda_0$, the azimuthal phase slope is not exactly 1, so the output mode is not a perfect LG_{01} beam.

Because real FEL heater lasers have finite spectral bandwidth, the SPP dispersion introduces azimuthal phase errors that can change the donut shape and reduce the contrast of the dark core. This will modify the transverse pattern of the energy modulation $\Delta\gamma(r, \theta)$ seen by the electrons and can make the final energy distribution less Gaussian. In this paper, we use Gaussian-beam and vortex-beam theory [4] to derive the dispersion factor of the SPP, analyze the OAM-mode content, and see how these effects influence an LG_{01} heater in an FEL.

METHODS

In this section, we describe how the spiral phase plate (SPP) creates the phase we need for the LG_{01} beam, and how dispersion changes this phase at different wavelengths. All math steps are kept the same, but we explain them in a simpler way.

We study an $l = 1$ SPP made of fused silica. Its thickness changes with angle as

$$t(\theta) = t_0 + \frac{\Delta t}{2\pi}\,\theta, \tag{2}$$

where t_0 is just a constant offset, and Δt is the total height difference after one full rotation. Putting Eq. (2) into the phase expression in Eq. (1), the phase added at wavelength λ becomes

$$\phi(\theta, \lambda) = \frac{2\pi}{\lambda}\,[n(\lambda) - 1]\left(t_0 + \frac{\Delta t}{2\pi}\,\theta\right). \tag{3}$$

For the SPP to give a perfect 2π phase twist at the design wavelength λ_0, we need the condition $\phi(2\pi, \lambda_0) = 2\pi$. This directly gives

$$[n(\lambda_0) - 1]\,\frac{\Delta t}{\lambda_0} = 1, \tag{4}$$

so the required height difference is

$$\Delta t = \frac{\lambda_0}{n(\lambda_0) - 1}. \tag{5}$$

Once Δt is fixed, we can look at what happens at wavelengths that are not λ_0. At $\lambda \neq \lambda_0$, the phase becomes

$$\phi(\theta, \lambda) = \frac{2\pi}{\lambda}\,[n(\lambda) - 1]\,\frac{\Delta t}{2\pi}\,\theta = 2\pi D(\lambda)\,\theta, \tag{6}$$

where we define the dispersion factor

$$D(\lambda) = \frac{n(\lambda) - 1}{n(\lambda_0) - 1}\,\frac{\lambda_0}{\lambda}. \tag{7}$$

If $D(\lambda) = 1$, the SPP works perfectly and we get the ideal LG_{01} phase. If $D(\lambda) \neq 1$, the azimuthal phase slope changes, and the output field becomes

$$E(r, \theta, \lambda) = A(r)\exp\big[iD(\lambda)\theta\big], \tag{8}$$

where $A(r)$ is the radial envelope of the beam determined by the input Gaussian mode and the SPP transmission. [4] The phase error compared to the perfect vortex is

$$\delta\phi(\theta, \lambda) = \theta\,[D(\lambda) - 1]. \tag{9}$$

To actually compute $D(\lambda)$, we need a model for the refractive index $n(\lambda)$. For fused silica, we use the Sellmeier equation [5]

$$n^2(\lambda) = 1 + \frac{B_1\lambda^2}{\lambda^2 - C_1} + \frac{B_2\lambda^2}{\lambda^2 - C_2} + \frac{B_3\lambda^2}{\lambda^2 - C_3}, \tag{10}$$

where B_i and C_i are known constants, and λ is in micrometers. We choose $\lambda_0 = 800\ \mathrm{nm}$ (the typical heater wavelength) and evaluate $D(\lambda)$ over a small range of $\lambda_0 \pm 3\ \mathrm{nm}$, which corresponds to a realistic infrared laser bandwidth.

OAM-mode expansion

Once we know $D(\lambda)$, we study how the field $\exp[iD(\lambda)\theta]$ breaks into different orbital-angular-momentum (OAM) modes. We expand it as

$$\exp(iD\theta) = \sum_{m=-\infty}^{\infty} c_m(\lambda)\, \exp(im\theta). \tag{11}$$

Using the orthogonality of the exponential functions, we find that

$$c_m(\lambda) = \frac{1}{2\pi}\int_0^{2\pi} \exp\bigl[i(D-1)\theta\bigr]\, \exp(-im\theta)\, d\theta, \tag{12}$$

which becomes

$$c_m(\lambda) = \operatorname{sinc}\bigl[\pi(D(\lambda)-1-m)\bigr]. \tag{13}$$

When $D = 1$, we get a pure LG_{01} beam: $c_1 = 1$ and all other $c_m = 0$. When D deviates slightly, we write $D = 1+\varepsilon$ and use a small-error expansion:

$$|c_1|^2 \approx 1 - \frac{\pi^2}{3}\varepsilon^2, \tag{14}$$

$$|c_0|^2 \approx \frac{\varepsilon^2}{4}, \tag{15}$$

$$|c_2|^2 \approx \frac{\varepsilon^2}{4}. \tag{16}$$

This shows that even very small dispersion ($\varepsilon \sim 10^{-2}$) already sends some power into the $m = 0$ and $m = 2$ modes.

Donut distortion model

To understand how OAM leakage affects the LG_{01} intensity, we approximate the LG_0^1 mode as [4]

$$I_{01}(r) \propto \left(\frac{r}{w_0}\right)^2 \exp\left(-\frac{2r^2}{w_0^2}\right). \tag{17}$$

This mode has a dark core at $r = 0$. When dispersion causes leakage, the field becomes a sum of LG_{01}, LG_{02}, and LG_{00}:

$$E(r,\theta) \approx c_1\, \mathrm{LG}_{01}(r,\theta) + c_2\, \mathrm{LG}_{02}(r,\theta) + c_0\, \mathrm{LG}_{00}(r,\theta). \tag{18}$$

The intensity is therefore

$$\begin{aligned} I(r,\theta) &= |E|^2 \\ &\approx |c_1 \mathrm{LG}_{01}|^2 + |c_2 \mathrm{LG}_{02}|^2 + |c_0 \mathrm{LG}_{00}|^2 + 2\,\mathrm{Re}\bigl[c_1 c_2^* \mathrm{LG}_{01} \mathrm{LG}_{02}^* e^{i\theta}\bigr] + \dots \end{aligned} \tag{19}$$

Because LG_{02} and LG_{00} both have intensity at the center, they partially fill the dark core. The interference term with $e^{i\theta}$ causes azimuthal "lumpiness" in the donut.

Numerical procedure

To visualize these effects, we compute $D(\lambda)$ using Eqs. (10) and (7) over the range $\lambda_0 \pm 3$ nm for fused silica. This gives $\varepsilon(\lambda) = D(\lambda) - 1$, which we use to estimate OAM leakage.

For donut distortion, we use a simple radial model in MATLAB. We approximate the radial envelopes of LG_{01} and LG_{02} as

$$\mathrm{LG}_{01}(r) \propto \left(\frac{r}{w_0}\right) \exp\left(-\frac{r^2}{w_0^2}\right), \tag{20}$$

$$\mathrm{LG}_{02}(r) \propto \left(\frac{r}{w_0}\right)^2 \exp\left(-\frac{r^2}{w_0^2}\right), \tag{21}$$

take $w_0 = 1$ (normalized), set $c_1 \approx 1$ and $c_2 \approx \varepsilon$ for $\varepsilon = 0, 0.01, 0.02$, and compute

$$I(r) = \left|c_1 \mathrm{LG}_{01}(r) + c_2 \mathrm{LG}_{02}(r)\right|^2. \tag{22}$$

This model clearly shows how dispersion fills in the center and changes the donut shape.

RESULTS AND INTERPRETATION

Figure 1 below shows the dispersion factor $D(\lambda)$ for fused silica with $\lambda_0 = 800$ nm. In the range ± 3 nm, $D(\lambda)$ differs from 1 by up to about 1.2×10^{-2}, i.e. $\varepsilon \sim 0.012$ at the spectrum edges. This size of deviation matches typical near-infrared dispersion in silica. [5]

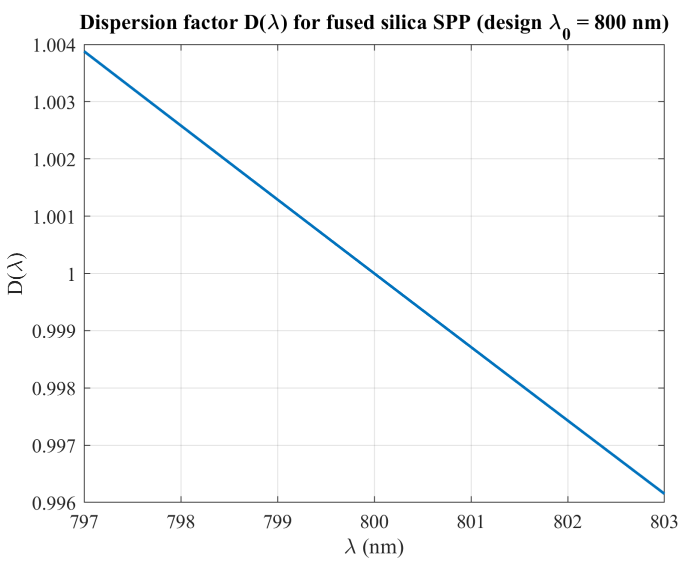

Figure 1: Dispersion factor $D(\lambda)$ for a fused-silica SPP with design wavelength $\lambda_0 = 800$ nm, evaluated over a ± 3 nm range using the Sellmeier model. [5]

Using $\varepsilon \approx 0.012$ in the small-error formulas, we obtain

$$|c_2|^2 \approx \frac{\varepsilon^2}{4} \approx 3.6 \times 10^{-5}, \qquad |c_0|^2 \approx 3.6 \times 10^{-5}.$$

Even though these numbers are small, they still affect the LG_{01} pattern. The reason is that LG_{02} and LG_{00} already have light at the center. When we superpose LG_{01} and LG_{02}, the dark core is partly filled and the donut ring becomes broader and less symmetric.

In our simple radial model, Figure 2 below shows the intensity profiles for $\varepsilon = 0, 0.01, 0.02$. For $\varepsilon = 0$, there is a deep minimum at the center and one clean ring. For $\varepsilon = 0.01$, the center rises to a few percent of the maximum and the ring becomes wider. For $\varepsilon = 0.02$, the center is even brighter and the ring shape is more distorted. These results agree with the interference picture between LG_{01} and LG_{02}.

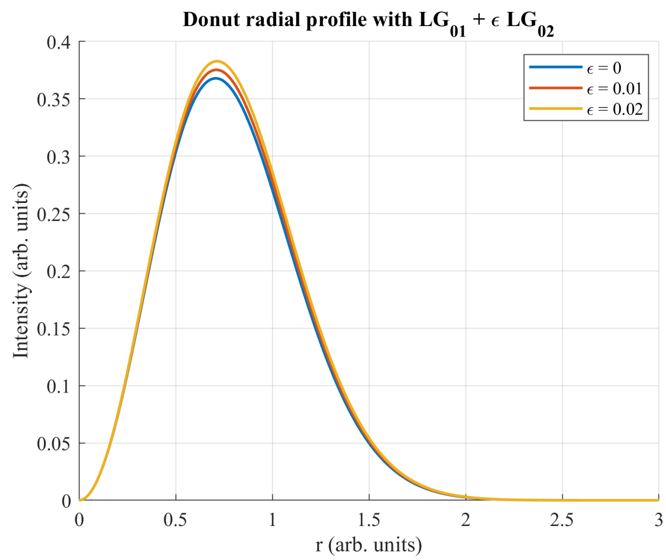

Figure 2: Radial intensity profiles for the LG_{01}+LG_{02} superposition model at different dispersion errors $\varepsilon = 0, 0.01, 0.02$. Increasing ε leads to central filling and ring distortion.

For the LG_{01} heater studied by Tang et al., these distortions directly change the transverse pattern of $\Delta\gamma(r, \theta)$. In the best case, $|E(r)|$ grows almost linearly with r near the axis and is symmetric in angle. When $m = 0$ and $m = 2$ components appear, $|E|$ becomes angle-dependent, so electrons at the same radius but different θ get different energy kicks. At the same time, the filled-in center reduces the difference between on-axis and off-axis electrons. Together, these effects move the induced energy distribution away from a clean Gaussian and can reduce how well the heater suppresses microbunching. [1–3]

CONCLUSION

Tang et al. showed that LG_{01} laser heaters can strongly improve microbunching suppression by generating smooth, almost Gaussian energy distributions. [1] In this paper, we used Gaussian-beam and vortex-beam theory [4, 5] to look more carefully at one part of their setup: the spiral phase plate and its material dispersion.

We derived a dispersion factor $D(\lambda)$ that tells us how the SPP phase deviates from the ideal $\phi(\theta) = \theta$ when the wavelength is not λ_0. By expanding the field into OAM modes, we obtained expressions for $c_m(\lambda)$ and showed that even a small deviation ($\varepsilon \sim 10^{-2}$) already causes leakage into LG_{00} and LG_{02}. Our simulations support this and show that the donut core fills in and the ring gets distorted.

For FEL laser-heater design, this means that a simple SPP-based LG_{01} generator is not always enough when the laser has finite bandwidth. If we want higher mode purity over a larger spectrum, it may be better to use other vortex-beam elements that are more achromatic, such as q-plates, metasurfaces, or spatial light modulators. These devices could help keep the LG_{01} profile cleaner and further improve microbunching suppression in future FELs.

REFERENCES

References

[1] J. Tang *et al.*, "Laguerre-Gaussian mode laser heater for microbunching instability suppression in free-electron lasers," *Phys. Rev. Lett.* **124**, 134801 (2020).

[2] Z. Huang and K.-J. Kim, "Formulas for coherent synchrotron radiation microbunching in a bunch compressor chicane," *Phys. Rev. ST Accel. Beams* **5**, 074401 (2002).

[3] E. Saldin, E. Schneidmiller, and M. Yurkov, "Longitudinal space charge-driven microbunching instability in the TESLA Test Facility linac," *Nucl. Instrum. Methods Phys. Res. A* **490**, 1–8 (2002).

[4] J.-M. Liu, *Principles of Photonics* (Cambridge University Press, 2016).

[5] M. Born and E. Wolf, *Principles of Optics*, 7th ed. (Cambridge University Press, 1999).